

Performance of 10 - 100 GeV gamma ray camera for SUBARU optical-infrared telescope

A. Asahara^a, Y.Komiyama^b, G.Kosugi^b, H.Kubo^a, S.Miyazaki^b,
M.Mori^c, M.Nakagiri^b, D.Nishida^a, R.Ogasawara^b, R.Orito^a,
K.Sakurazawa^d, T.Takata^b, T.Tanimori^a, and T.Usuda^b

^aDepartment of Physics, Kyoto University,
kitashirakawa Oiwakecho, Kyoto 606-8502, Japan

^bSubaru Telescope, National Astronomical Observatory,
650 North Aohoku Place, Hilo, HI 96720.

^cICRR, University of Tokyo,
5-1-5 Kashiwa-no-ha, Chiba 277-8582, Japan

^dTokyo Institute of Technology,
2-12-2 Ohokayama, Meguro-ku, Tokyo 152-8551, Japan

ABSTRACT

We developed the gamma-ray camera for the SUBARU infrared-optical telescope,¹ named “CheSS” (Cherenkov light detecting System on Subaru). CheSS was designed based on the Imaging Atmospheric Cherenkov Technique (IACT) which has been established by detections of high energy gamma-ray sources in the last decade. According to our Monte Carlo simulation, the energy threshold of CheSS for the Crab is 30 GeV at zenith angle of 10 degrees, and the expected sensitivity for the unpulsed component can reach $\sim 10\sigma$ level and more for pulsed one during 10 hours of on-source pointing.

Keywords: Gamma-ray pulsar, Crab, IACT, DAQ

1. INTRODUCTION

In the last decade, gamma-ray detectors have made remarkable progress and given us exciting view of our universe. Below ten GeV, Compton Gamma Ray Observatory (CGRO) revealed high energy phenomena,² and above 100 GeV, ground-based detectors using the Imaging Atmospheric Cherenkov Technique (IACT) are working now.³ In the 10 GeV to 100 GeV region, however, only a few detectors have explored until now.

This energy region is quite important to study the emission mechanism of gamma-ray pulsars.⁴ There are two classes of models to explain high-energy pulsed emission from pulsars. One class of models, called “polar cap” models, assumes pulsed emission comes from high-energy electrons accelerated near the surface of a neutron star. The other class, called “outer gap” models, postulates it comes from such electrons accelerated in potential gaps between open field lines of magnetic field and a neutral sheet in the outer magnetosphere of a pulsar. Both two types of models can explain the wide-band pulsed emission below the GeV region fairly well, but they predict clearly different behaviors above the 10 GeV region: gamma-rays produced near the neutron star surface in polar cap models are lost due to electron-positron pair creation in the strong magnetic field, while gamma-rays generated off the neutron star do not suffer such losses. Thus polar cap models predict very steep cutoff at lower energies than those predicted in outer gap models, which can be distinguished by observations in the 10 GeV to 100 GeV range. Figure 1 shows two pulsar models and observation results of various detectors on Crab pulsar, which is the most famous gamma-ray pulsar and the standard candle for gamma-ray astronomy.

Observing the gamma-ray spectrum in this energy region has been proved to be elusive to both ground-based and satellite instruments. Satellite detectors have had too small collection areas to detect gamma-rays above 10

Correspondence: E-mail: asahara@cr.scphys.kyoto-u.ac.jp

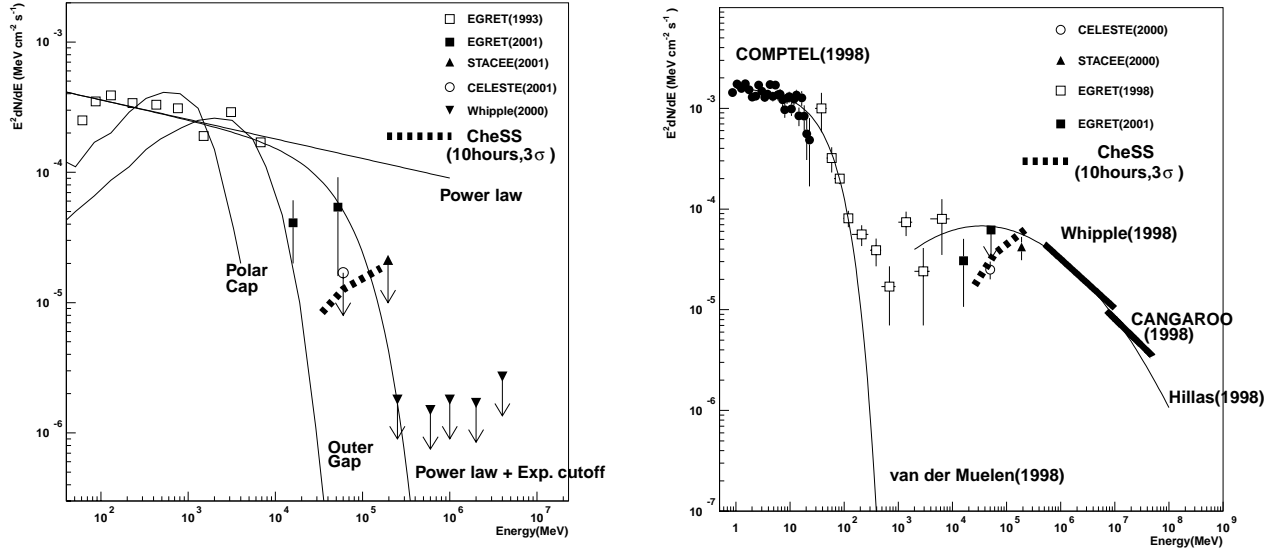


Figure 1. The energy spectrum of the Crab. The left panel shows pulsed component^{6,7} and the right panel shows unpulsed component.⁸ Note that ‘EGRET (2001)’ points are based on rough estimate. Also shown are the expected 3 sigma sensitivities of CHESS in 10 hours of observation. Just only ON-OFF chopping (no imaging analysis) enables to detect 30 GeV gamma-ray from Crab pulsar/nebula.

GeV. On the other hand, although ground-based detectors can achieve large collection areas, it is difficult for them to detect Cherenkov light caused by gamma-ray showers below 100 GeV since the photon density is too small. According to our simulation, however, Cherenkov light density caused by cosmic rays is 4 times larger at high altitude (4000m) than at sea level (described in detail in section 4). This result means that “high altitude” and “large mirror” enable us to observe the 10 GeV energy region. The SUBARU optical-infrared telescope is located on the top of Mt. Maunakea, altitude 4200m. Our gamma-ray camera, named “CheSS” (Cherenkov light detecting System on SUBARU), was designed to investigate this unexplored region with SUBARU’s 8.2m fine mirror.

Bertsch et al.(2001) presented a list of photons above 10 GeV detected by EGRET on board CGRO.⁵ The two highest-energy events were reported to be above 100 GeV and a rough estimate of their flux contradicts the upper limits reported by CELESTE, a wide-area non-imaging Cherenkov telescope operated by a French group⁶ (Fig. 1). However, considering the small number of events detected by EGRET at this energy range and possible systematic error of the energy calibration of CELESTE, it is clear that we need more observations. With CheSS working in the 30 to 100 GeV energy range we can clarify the emission mechanism of pulsars and can provide information of the pulsar magnetosphere.

2. ELECTRONICS AND DATA ACQUISITION

2.1. Electronics

Size, weight, and power consumption of instruments at the SUBARU prime focus are severely restricted. CheSS designed for the prime focus is one of the most compact detectors among instruments of SUBARU. The chassis is cylindrical in shape with base radius of 0.5m, height of 1m, weight of about 200kg, and the power consumption

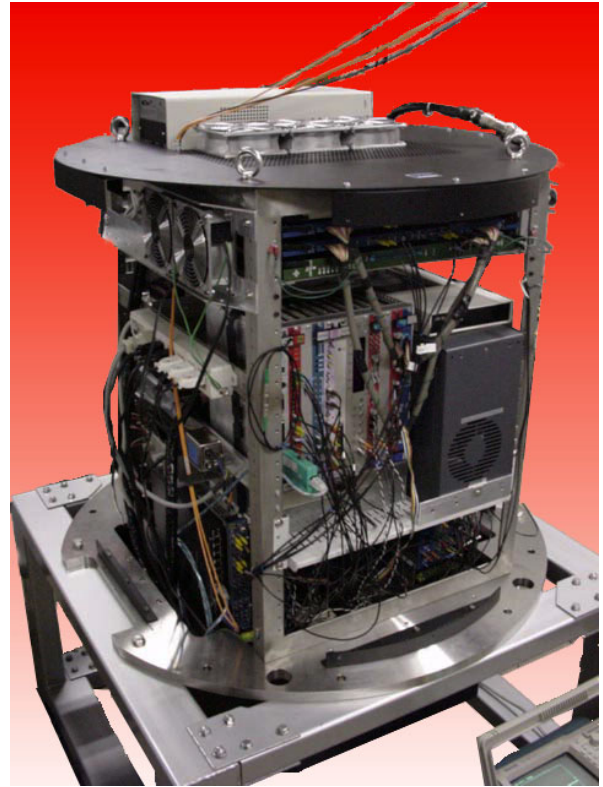
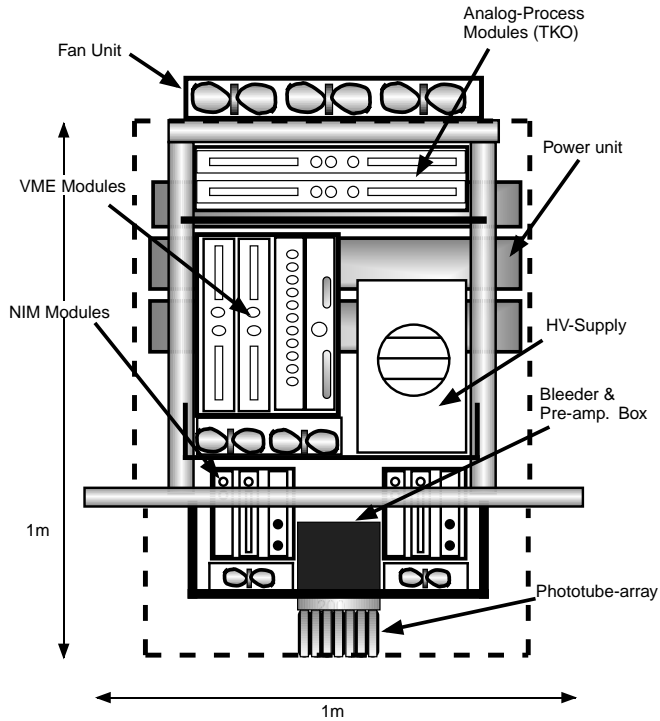


Figure 2. CheSS Overview.

is under 700W (Fig. 2). Electronics use the DC power line supplied by six low-noise switching power supplies inside CheSS. The main power line (AC120V) and optical fiber cables for networking (10Base-T), are provided by the SUBARU Prime Focus Unit (PFU). PFU was designed for “Suprime-cam”⁹ which is the optical imaging detector on the SUBARU prime focus and one of the seven main detectors. CheSS is also installed in PFU, which has the correction lenses for aberrations, but they have enough transmittance for Cherenkov light photons (85% over 400nm, 50 % for 350nm).¹⁰

Figure 3 shows an overview of the electronics . Half of authors are the members of the CANGAROO project, and the basic concept is similar to the CANGAROO 10m telescope¹¹ using IACT, located in Woomera, Australia. The focal plane detector consists of an array of 44 separate photomultiplier tubes (PMTs) (Fig. 4), and covers a field of view of $0.75^\circ \times 0.75^\circ$. This PMT (Hamamatsu 2497UV) is sensitive to photons between 350nm and 450nm, and its quantum efficiency is about 20 % in this region. The size of the photo-cathode is 23mm \times 23mm in square shape, without light guides. High voltages are applied to blocks of 5 PMTs from the supply (LeCroy 1451) which is remote-controlled via an optical-RS232C converter. The high voltage values are around -1500V, but slightly different from block to block in order to equalize PMT gains whose average value is about 4×10^5 .

Signals from PMTs are amplified in AMP-BOX which consists of amplifier chips (LeCroy TRA402S), and sent to Discriminator & Summing Modules (DSMs). DSM was originally developed for the CANGAROO telescope, and it has multi functions useful for IACT (Fig. 5). In the DSM, signals from each PMT are amplified with fast shaping amplifiers, and fed to two independent discriminators. One is an updating discriminator for measuring the hit timings by Time to Digital Converters (CAEN V667), and the other is non-update discriminator whose digital output is counted by 12bit scaler, and used for the event trigger logic which we call as “LSUM”. Its pulse width is set to be about 20nsec, to cover the time dispersion of Cherenkov light photons

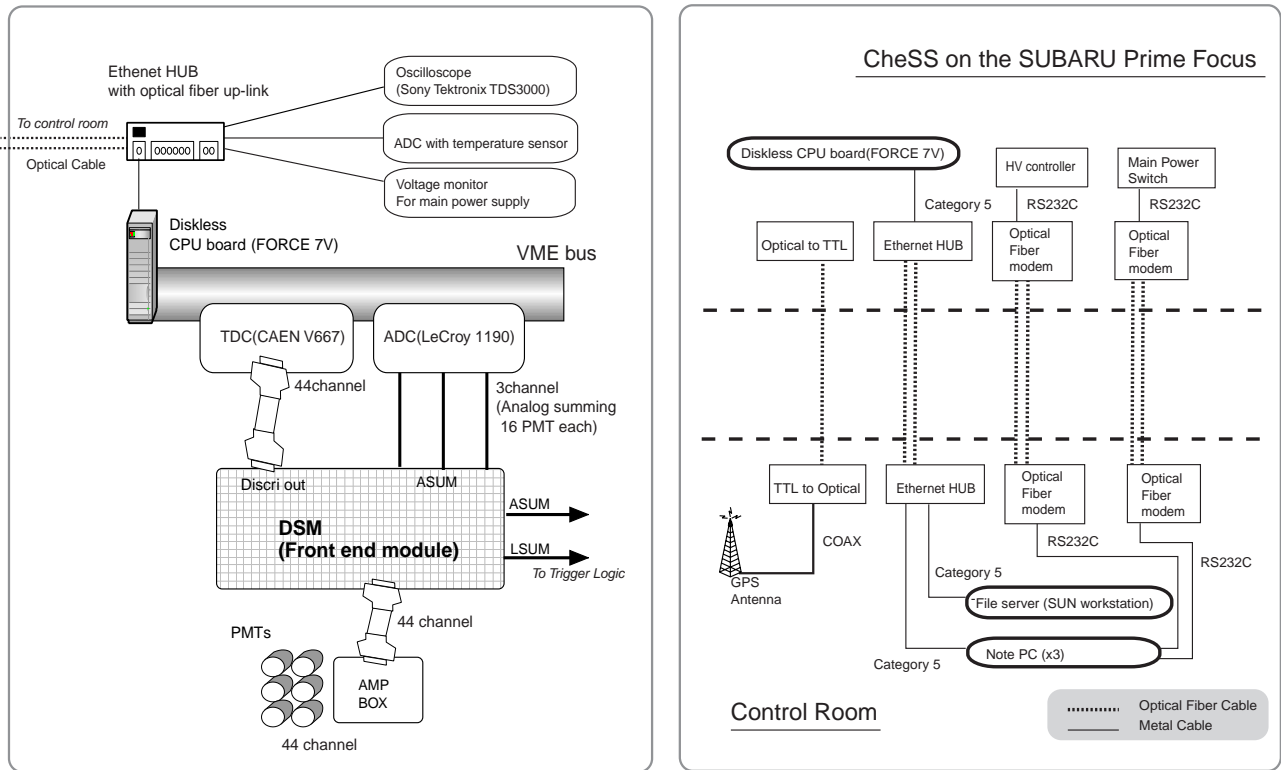


Figure 3. Left panel: Diagram of electronics inside CheSS. The CPU board controls all the electronics, readouts the data in the memory of VME modules, and sends it to the file server. Right panel: Diagram of connection between CheSS and Control room.

emitted by air showers. Moreover, DSM outputs the summed signal of 16 channel (hereafter “ASUM”). ASUM signals are also used for the trigger logic. Setting the thresholds of two discriminators and readout of 12bit scaler data are conducted via the VME bus.

The data acquisition trigger scheme is shown in Fig. 5. LSUM signals from DSMs are summed, and discriminated to determine how many PMTs hit at the same time. On the other hand, ASUM signals are also summed, and discriminated to determine how much number of photoelectrons are detected. Thresholds of these two discriminators (CAEN V253) are adjustable via VME-bus. The coincidence of both discriminator outputs becomes the event trigger. In order to check the DAQ system, a pulse from a GPS receiver is added to a DAQ trigger every second. This is how we can put a trigger condition, such as “Trigger when 2PMTs detects 3 photoelectrons simultaneously”.

The main measurement device of CheSS is TDC for each PMT channel. TDC records rising and falling time of PMT signals. Its time resolution is 0.75nsec, and time window is 840ns. CheSS does not use Analog to Digital Converters (ADC) for each PMT signal, but we can estimate the number of photo-electron using TDC width (see section 2.3). As an additional measurement device, charge integration ADC (Lecroy 1182) is equipped and measures three ASUM signals from DSMs.

Time information is quite important for detecting pulsed component of the Crab pulsar. CheSS has three independent clocks. The first clock is the CPU system time, which is adjusted by Network Time Protocol server via Ethernet. The second clock is the 1MHz quartz oscillator. The third and the most accurate clock is the GPS signal receiver. A VME latching scaler (CAEN V830) counts GPS 1pps pulses and 1MHz oscillator pulses and latches when an event trigger occurs.

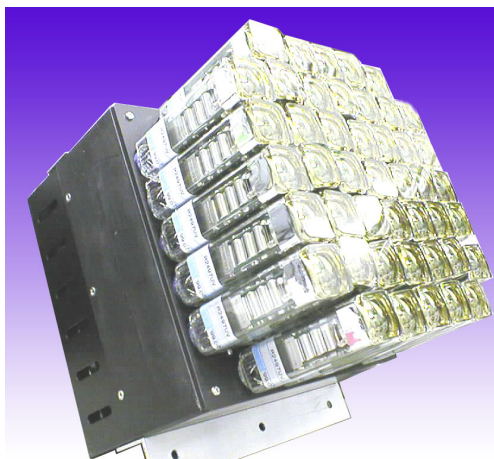


Figure 4. Photo Multiple Tube array which covers a field of view $0.75^\circ \times 0.75^\circ$. The size of each PMT is 26mm \times 26mm (the photo-cathode is 23mm \times 23mm). The black box behind PMTs is AMP-BOX which consists of amplifier chips (LeCroy TRA402S).

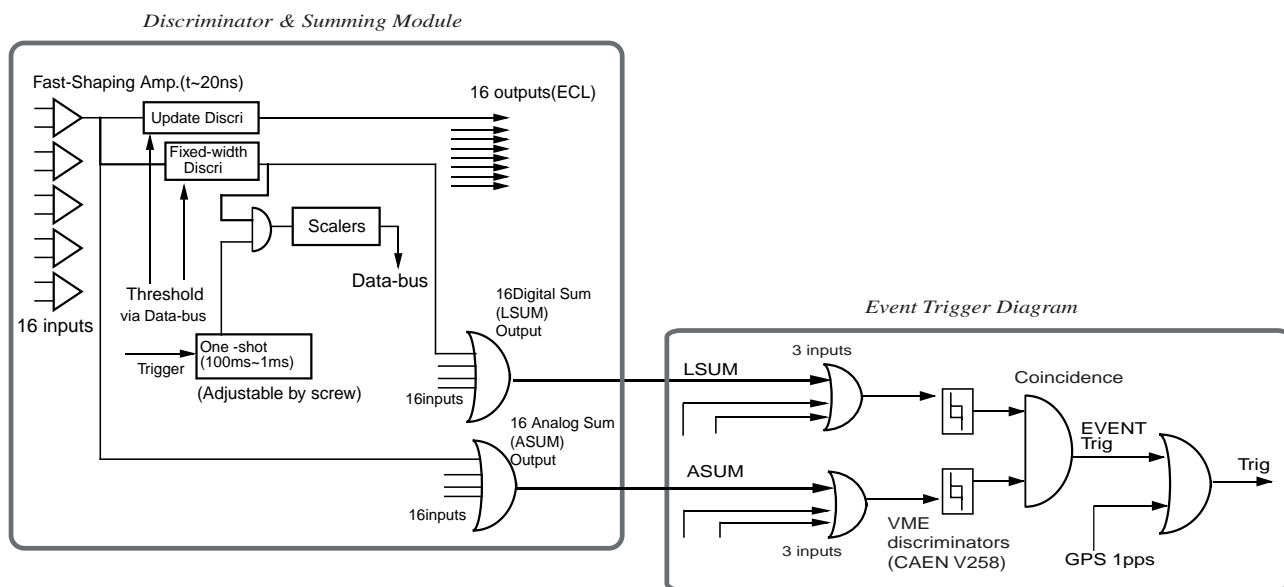


Figure 5. The diagram of Discriminator & Summing Module (DSM) and Event trigger logic. Threshold for update discriminators and fixed-width discriminators (non-update) are set by the diskless CPU board via VME-bus. The 12bit scaler data is also read out via VME-bus.

2.2. Data Acquisition

CheSS and the control room are networked using 10Base-T Ethernet. VME-bus CPU board (FORCE 7V) inside CheSS controls all electronics except high voltage modules*, readouts the digital data from fast VME-bus modules, and sends it to control room via optical fiber cables (Fig. 3 right panel). In the control room, a file server of CPU receives the data and sends all commands necessary for observations are sent to the CPU inside CheSS.

The environment inside the astro-dome is quite severe for a hard disk. The air temperature is always near 0 °C, and the telescope is always moving to track the target. Therefore, a VME board CPU cannot use a hard disk. Instead, it mounts a system disk via NFS (Network File System) from a file server located in the control room. This is so called “diskless client - file server” system. The NFS system is secure, but the trade-off is the performance of data acquisition speed. In this case, however, it does not matter since the data size of CheSS is quite small, about 500 Byte per event. According to our test of the data acquisition performance, CheSS CPU can deal with event triggers at 300Hz with dead time of 20% (Fig. 6).

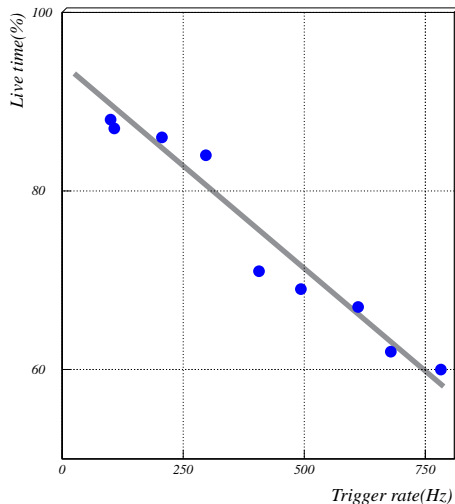


Figure 6. The data acquisition speed of CheSS.

2.3. Calibration using LED

The number of photoelectrons detected with CheSS is estimated using the width of TDC data (Fig. 7). We calibrated the TDC width vs. ADC channel using a blue LED (Nichia NSPB320BS). The result of this calibration is shown in Fig. 7. The ADC channel has linear correlation with the number of photoelectron. In this case, one photoelectron is estimated to be about 35 ADC channel.

3. OBSERVATION OF CRAB PULSAR/NEBULA

The SUBARU telescope equipped with CheSS was pointed in the direction of the Crab pulsar/nebula on 17th, 18th, and 19th December 2001. Total observation time was about 24 hours for on-source and off-source runs.

At first, we conducted operation test using LED. Figure 8 shows the distribution of TDC start-timing in a LED calibration run with the dome of SUBARU closed. In this run, we can see only a spike around 700 channel

*On the point of security, another independent PC controls high voltage modules via optical-RS232C converter.

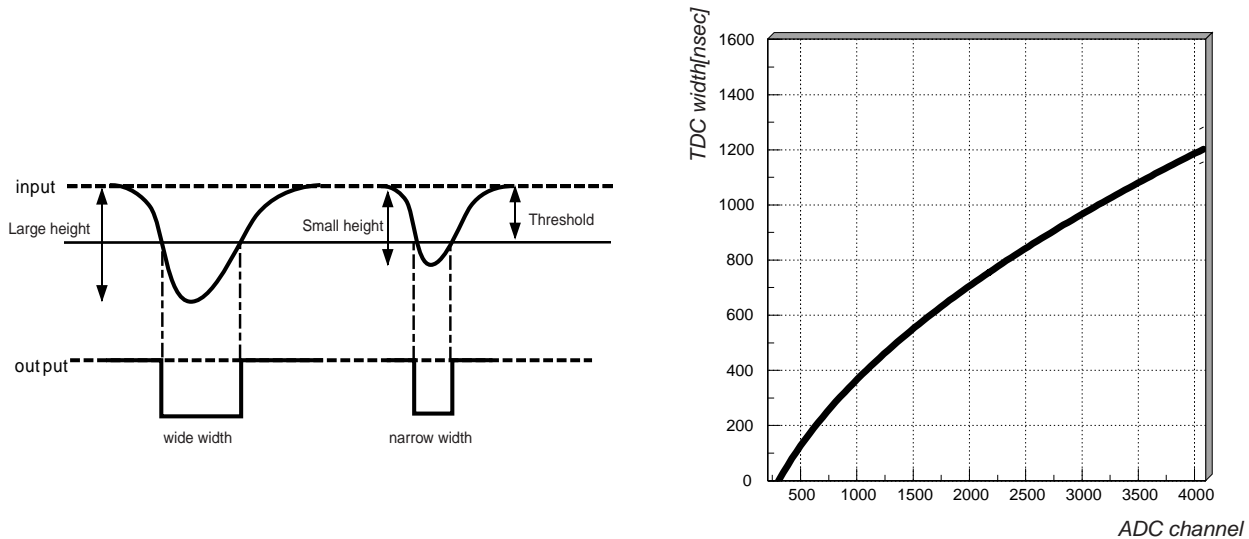


Figure 7. TDC width (hit over threshold) calibration. The number of photo-electrons detected with CheSS is estimated using the width of TDC data. Left panel shows the concept of this method. Right panel shows the result of the calibration.

because there is no night sky background. In the same LED calibration run with the dome opened, the data shows a spike caused by trigger signal and a flat component attributed to the night sky background.

The noise reduction effect is shown in Figure 8. The top right-hand panel shows a raw TDC distribution on 18 December 2001. The spike at about 700 channel means triggered signals. And other hits, - from 0 to 650 channel, and from 880 to 1120 channel -, are due to the night sky background. On the other hand, the bottom right-hand panel shows the distribution of TDC start-timing of the events which exceeds 3000 ADC channel (ADC cut). This is one of the simplest cut. Nevertheless, we can find clearly that the night sky background is reduced. In the observation data, the width of the spike is about 20nsec, and this value is consistent with typical propagation time of an air shower and electronics. SUBARU main mirror is near parabolic shape, and the time propagation of an air shower can be reproduced with high accuracy. Thus, we use only spikes around 700 channel for analysis, and discard others (Timing cut). Now the data analysis for this reduced data is underway.

4. MONTE CARLO SIMULATION

We have simulated air showers generated by gamma-rays, protons, and electrons using CORSIKA¹² which is a detailed Monte Carlo program to study the evolution and properties of extensive air showers in the atmosphere. We began by considering the nature of Cherenkov light at high altitude.

Figure 9 shows the light density distribution at various altitudes. At 4000m, the light density is 4 times larger than at sea level. This fact suggests that 10m-class mirrors at 4000m allow us to detect faint Cherenkov light caused by particles in the 10 GeV region.

Nowadays, there are many 10m-mirrors at high altitude in Hawaii or Chile, but most of optical or infrared telescopes have too small field of view (FOV) for IACT. In general, IACT needs large FOV, at least 1 degree, in order to apply the imaging analysis for the reduction of the night sky background and protons. The SUBARU telescope among 10m-mirrors has the largest FOV of 0.75 degree at its primary focus. This field of view is not

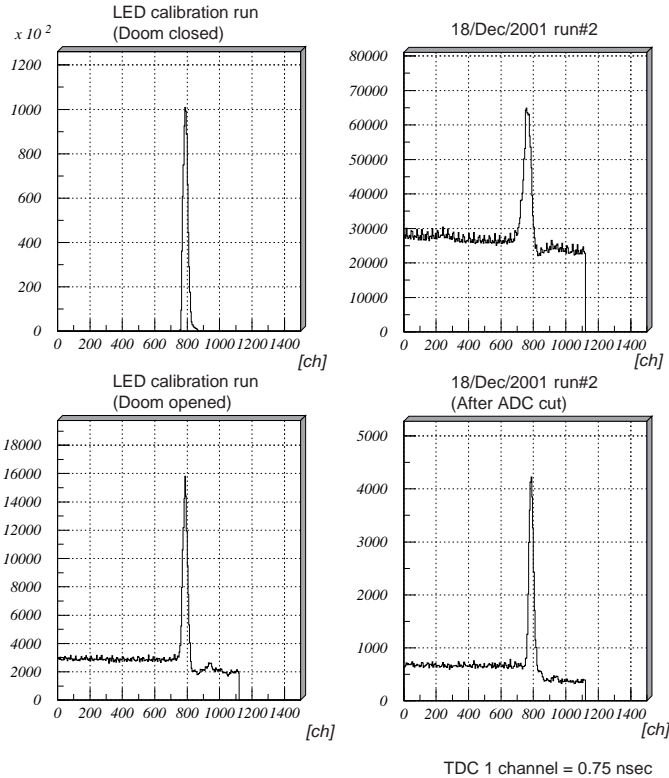


Figure 8. Distribution of hit timing of PMTs. Top left-hand: LED calibration run during the dome closed. Bottom left-hand: LED calibration run during the doom opened. Top right-hand: Raw data taken in the sky observation without LED. Bottom right-hand: Same data after ADC channel cut (3000ch).

large enough to apply the detailed image analysis, such as CANGAROO and Whipple,¹³ but it is the largest among existing optical or infrared telescopes. Even if FOV is relatively small, a Cherenkov light image at high altitude is concentrated to the center of FOV, and its size becomes smaller than at sea level. Moreover, at high altitude, Signal to Noise ratio is estimated to be over 0.05 in the case of the Crab pulsar/nebula. Thus, the rough image analysis and chopping observations between on-source and off-source enable us to detect 30GeV gamma-ray from the Crab pulsar/nebula.

At first, we calculate how much the night sky background is detected by CheSS. According to Jelley's data,¹⁴ the night sky background is expected to be about 6 photoelectrons per event. In this calculation, we use following parameters: FOV is 0.75deg, Focal length is 15m, and Mirror diameter is 8.2m. Moreover, the wavelength dependency of the quantum efficiency of PMTs, reflectivity of mirror,¹⁵ and transmittance of correction lens,¹⁰ are taken into account.

Secondly, we simulated the expected energy spectrum of SUBARU with CheSS under the night sky background, shown in Fig. 10 (triangle). In this simulation, we used the extrapolated flux of the Crab pulsar/nebula,¹⁶ and the observed fluxes of electrons¹⁷ and protons.¹⁸ Then we set the trigger condition, "Trigger when 2PMTs detects 3 photo-electrons simultaneously", which is the same as the observation. Expected trigger rate which is estimated from the energy spectrum is about 26.7 Hz for protons, 0.9 Hz for gamma-rays, 2.2 Hz for electrons. Thus the total trigger rate is about 30Hz which is consistent with the real observation data in December 2001.

Thirdly, in order to reduce the night sky background and improve the signal to noise ratio, we cut the events

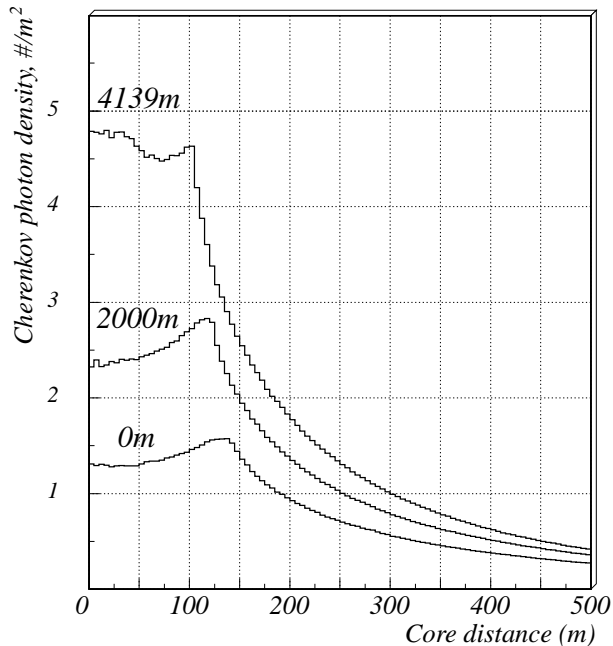


Figure 9. The density distribution of Cherenkov light photon caused by 10 GeV gamma-ray at high altitude. Distributions are averaged over 1000 showers.

if the sum of photo-electrons is under 7 photoelectrons. After this cut, we obtained the energy spectrum shown in Fig. 10 (circle). This is not a strong cut, and we estimate the energy threshold for gamma-ray flux is about 30 GeV for the Crab pulsar/nebula. The total expected number of gamma-rays in 10hours observation is 8×10^3 counts (backgrounds - proton and electron - are 2.5×10^5 counts in total). Thus, the expected sensitivity for the unpulsed component can reach $\sim 10\sigma$ level and more for pulsed one for 10 hours of on-source pointing (Fig. 1). In the actual analysis, more artful cuts will be applied, and the signal to noise ratio will be improved. The energy threshold for protons is about 90 GeV which is higher than that of gamma-rays. This is because the number of Cherenkov photons produced by protons is 3 - 10 times (depends on the energy of seed) smaller than that by gamma-rays.

In Dec 2001, we observed the Crab pulsar/nebula and three different points which are 5, 10 and 12 minutes away from the Crab pulsar/nebula in order to measure the background. Trigger rate at each OFF point were distributed between 7 Hz and 35Hz since it depends on the condition of the night sky background. The trigger rate caused by air showers, however, should be the same at any points if the points have the same elevation angle. Figure 11 shows the distribution of total ADC channel for each event. We can see the hump around 2000 channel which is attributed to the night sky background. It is quite natural to use the data over 2300 channel to eliminate the night sky background (“ADC cut”). If we can reject the night sky background, trigger rate at three different points should be same value. After the ADC cut, trigger rate became 6.5 ± 2.5 Hz. According to the simulation, the trigger rate after the night sky background cut is 6.9 Hz (6.7Hz for protons and 0.2 Hz for electrons: See Fig. 10), which is consistent with the observation.

5. SUMMARY

We developed the gamma-ray camera for the SUBARU prime focus, named “CheSS”, which is the quite compact detector with a volume of 1 m^3 , using Imaging Atmospheric Cherenkov Technique. The main electronics consist of fast VME-bus modules, and controlled by on board diskless CPU which is connected to a file server in the control room via 10Base-T network. The data-size of CheSS is small (about 500 Byte/event), and the available trigger rate is about 300 Hz. According to our simulation, CheSS can detect gamma-rays in the 30 - 100 GeV

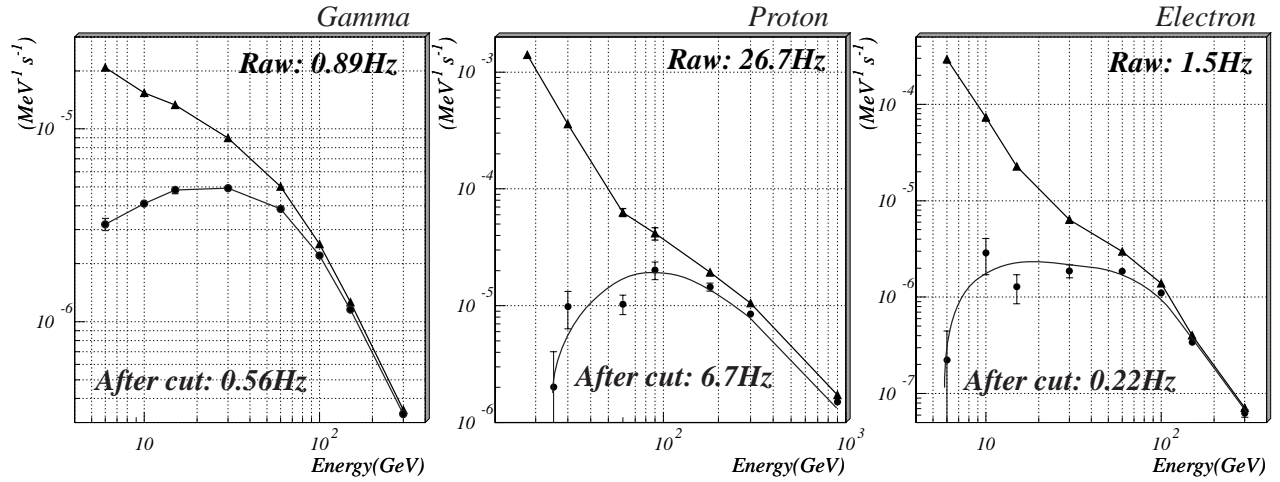


Figure 10. Expected energy spectrum of SUBARU with CheSS under the night sky background. Left panel: gamma. Middle panel: proton. Right panel: electron. Triangle points means expected energy spectrum without any cut. Circle points means expected energy spectrum after ADC cut to reject the night sky background.

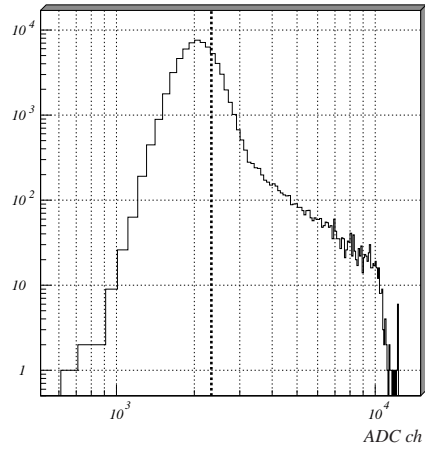


Figure 11. Distribution of total ADC channel for each event observed in December 2001. This figure was made from all off-source data over 20 degree of zenith angle. The dotted-line was used by “ADC-cut” (2300channel). The drop-off around 10000 channel is due to the saturation of hardware.

region. The expected sensitivity for the unpulsed component of the Crab nebula can reach $\sim 10\sigma$ level and more for pulsed one during 10 hours on-source pointing. On 17th, 18th, and 19th December 2001, the SUBARU telescope with CheSS was pointed in the direction of Crab pulsar/nebula. Total observation time was about 24hours(ON-OFF total). Now the data analysis is underway.

ACKNOWLEDGMENTS

The authors express their thanks to all the staffs of SUBARU telescope, NAOJ. A.A and R.O are financially supported by the Japan Society for the Promotion of Science. Part of this study was supported by the Yamada foundation.

REFERENCES

1. M. Iye and T. Yamashita, "Overview of Subaru instrumentation," in *Proc. SPIE Vol. 4008, p. 18-27, Optical and IR Telescope Instrumentation and Detectors, Masanori Iye; Alan F. Moorwood; Eds., 4008*, pp. 18–27, Aug. 2000.
2. N. Gehrels *et al.*, "The Compton Gamma Ray Observatory.," *Scientific American* **269**, pp. C38–+, 1993.
3. R. A. Ong, "Very high-energy gamma-ray astronomy.," *Physics Report* **305**, pp. 93–202, 1998.
4. A. K. Harding, "Gamma-ray Pulsars: Models and Predictions," in *High Energy Gamma-Ray Astronomy*, pp. 115–+, 2001.
5. D. Bertsh *et al.*, "EGRET Gamma Rays Above 10GeV," in *Paper presented at Gamma 2001: Gamma-Ray Astrophysics, held 4-6 April, 2001 in Baltimore, MD., 2001*.
6. M. de Naurois *et al.*, "Measurement of the Crab Flux above 60 GeV with the CELESTE Cerenkov Telescope," **566**, pp. 343–357, Feb. 2002.
7. R. W. Lessard *et al.*, "Search for Pulsed TEV Gamma-Ray Emission from the Crab Pulsar," **531**, pp. 942–948, Mar. 2000.
8. A. Harding and O. De Jager, "Towards a Major Cherenkov Detector-V," p. 64, 1997.
9. S. Miyazaki *et al.*, "Characterization and mosaicking of CCDs and the applications to the SUBARU wide-field camera (Suprime-Cam)," in *Proc. SPIE Vol. 3355, p. 363-374, Optical Astronomical Instrumentation, Sandro D'Odorico; Ed., 3355*, pp. 363–374, July 1998.
10. Y. Komiyama, "private communication," tech. rep., SUBARU telescope, NAOJ, 2001.
11. M. Mori and The Cangaroo Collaboration, "Cangaroo-II and Cangaroo-III," in *Gamma 2001: Gamma-Ray Astrophysics, held 4-6 April, 2001 in Baltimore, MD. Edited by Steven Ritz, Neil Gehrels, and Chris R. Shrader. Also AIP Conference Proceedings, Vol. 587. Melville, NY: American Institute of Physics, 2001., p.927*, pp. 927–+, 2001.
12. D. Heck *et al.*, "Report **FZKA 6019**, Forschungszentrum Karlsruhe; http://www-ik3.fzk.de/~heck/corsika/physics_description/corsika_phys.html," 1998.
13. T. C. Weekes *et al.*, "Observation of TeV gamma rays from the Crab nebula using the atmospheric Cerenkov imaging technique," **342**, pp. 379–395, July 1989.
14. J. Jelley, *Cherenkov Radiation and its Applications*, Pergamon Press, 1958.
15. <http://www.naoj.org/Observing/Telescope/reflect.html>, "Subaru primary mirror reflectivity," tech. rep., SUBARU telescope, NAOJ, 2001.
16. J. M. Fierro *et al.*, "Phase-resolved Studies of the High-Energy Gamma-Ray Emission from the Crab, Geminga, and VELA Pulsars," **494**, pp. 734–+, Feb. 1998.
17. S. Torii *et al.*, "The Energy Spectrum of Cosmic-Ray Electrons from 10 to 100 GeV Observed with a Highly Granulated Imaging Calorimeter," **559**, pp. 973–984, Oct. 2001.
18. M. Boezio *et al.*, "The Cosmic-Ray Proton and Helium Spectra between 0.4 and 200 GV," **518**, pp. 457–472, June 1999.